Au-Ge Alloys for Wide-Range Low-Temperature On-Chip Thermometry

J.R.A. Dann,[1,*] P.C. Verpoort,[1] J. Ferreira de Oliveira,[1,2] S.E. Rowley,[1,2] A. Datta,[3] S. Kar-Narayan,[3] C.J.B. Ford,[1] G.J. Conduit,[1] and V. Narayan[1,†]

[1] *Cavendish Laboratory, University of Cambridge, J.J. Thomson Avenue, Cambridge, CB3 0HE, United Kingdom*
[2] *Centro Brasileiro de Pesquisas Físicas, Rua Doutor Xavier Sigaud 150, Rio de Janeiro, 22290-180, Brazil*
[3] *Department of Materials Science, University of Cambridge, 27 Charles Babbage Road, Cambridge, CB3 0FS, United Kingdom*

(Received 23 February 2019; revised manuscript received 5 July 2019; published 12 September 2019)

We present results for a Au-Ge alloy that is useful as a resistance-based thermometer from room temperature down to at least 0.2 K. Over a wide range, the electrical resistivity of the alloy shows a logarithmic temperature dependence, which simultaneously retains the sensitivity required for practical thermometry while also maintaining a relatively modest and easily measurable value of resistivity. We characterize the sensitivity of the alloy as a possible thermometer and show that it compares favorably with commercially available temperature sensors. We experimentally identify that the characteristic logarithmic temperature dependence of the alloy stems from Kondo-like behavior induced by the specific heat treatment it undergoes.

DOI: 10.1103/PhysRevApplied.12.034024

I. INTRODUCTION

Measuring the temperature (T) dependence of material properties is crucial in increasing our understanding of condensed-matter systems. It is also important for the control and measurement of electronic devices, particularly quantum devices, that operate at low T. Cooling materials to very low T has often revealed rich and unexpected physics with relevance for current and future technologies. Understanding and quantifying low-temperature phenomena requires effective thermometry across the entire T range of interest.

A limitation of present-day thermometry schemes is the absence of a single sensor spanning a broad T range without loss of sensitivity. It is therefore customary to use multiple thermometers, each of which is designed for use in different parts of the T range of interest. For example, in resistance- (R) based thermometry, in which T is inferred from the electrical resistance of a "thermistor," metallic or semiconducting sensors are used depending on the T range in question: high T is most conveniently measured with metallic thermistors, which, however, lose sensitivity below approximately 5 K, where R is dominated by temperature-independent impurity scattering. At low T, semiconducting thermistors (e.g., Ge, RuO_2, carbon glasses) are used, in which R increases as T is lowered with activated behavior, $R \sim \exp(\Delta/k_B T)$. Yet despite the high sensitivity that such thermistors offer, the rapidly increasing R can raise substantial issues with measurements that avoid self-heating of the thermometer.

A variety of other techniques are also available for thermometry at low T, such as nuclear-orientation thermometry [1], magnetic thermometry [2], shot-noise thermometry [3], Johnson-noise thermometry [4], Coulomb-blockade thermometry [5,6], capacitance thermometry [7], the use of lithographically-defined on-chip thermocouples [8–11], using noninvasive charge-sensing thermometers [12], and employing normal-superconductor-based tunnel junctions [13,14].

Here we present a thermistor that offers several of the individual advantages presented by these techniques: namely, (i) it is sensitive over a broad T range; (ii) its resistance remains easily measurable and small enough to allow efficient thermalization and avoid self-heating; and (iii) it can be lithographically patterned to reliably measure spatial temperature gradients and/or be fabricated on chips as part of microelectronic devices.

The thermistor we report is made of a Au-Ge alloy (Au_xGe_{1-x}) and might be suitable as a R-based thermometer that can operate over a wide T range from 0.2 to 200 K, and possibly even up to room temperature. In particular, we demonstrate that for a range of compositions R shows a logarithmic dependence on T across a range of 3 orders of magnitude. The material satisfies the following conditions: (i) the sensitivity (S) remains usably high between room temperature and 0.2 K, with S increasing with decreasing T; (ii) the absolute value of $R(T)$ remains sufficiently small

*jrad3@cam.ac.uk
†vn237@cam.ac.uk

that self-heating should be negligible and thermalization should not be an issue; (iii) the material is suitable for lithographic micrometer-scale fabrication and thus for use on chips as part of nanoscale devices, as well as on larger scales for use in other environments, such as cryogenic refrigerators; and (4) the linearity of R as a function of $\log T$ allows a relatively simple calibration.

II. METHODS

The Au_xGe_{1-x} alloy is fabricated into Hall-bar devices by a photolithography and lift-off technique. The required thicknesses of Ge and Au are thermally evaporated in separate layers and the Hall bars are then heated in a reducing environment of nitrogen and hydrogen at approximately 450 °C for 2 min before being rapidly cooled to room temperature within a few minutes, as shown in Fig. S1 [27] within the Supplemental Material. Finally, Ohmic Ti/Au contacts are deposited in a second photolithography step. The composition of the material is measured in two separate ways: (i) the thickness of each layer is measured with a crystal monitor during the evaporation and (ii) energy-dispersive-x-ray-spectroscopy measurements (see Fig. S2 [27]) are performed after the heat treatment. The compositions from the two methods are consistent within 0.2%. The Hall bars are approximately 1 mm long, 80 μm wide, and 200 nm thick. Several different substrates are successfully used; namely, silicon, sapphire, and GaAs. Unless otherwise stated, all measurements presented here are performed on samples deposited on silicon substrates. The results are not observed to be affected by the choice of the three substrates, and show the same main characteristics over multiple separate processing batches. Resistance measurements are performed with standard four-terminal low-frequency lock-in techniques. Unless otherwise stated, a frequency of 77 Hz is used and the excitation current is 1–100 nA. The measurements reported here are performed in three different cryostats with base temperatures of 0.05, 0.2, and 0.3 K. While the qualitative nature of the results is unaffected between cryostats, to make quantitative comparisons of the results (Fig. 1), we introduce multiplicative factors of 1%–2% in Fig. 1 to ensure that data from different cryostats fall on the same curve.

III. RESULTS AND DISCUSSION

Figure 1 shows the temperature characteristics of a $Au_{0.07}Ge_{0.93}$ film. Over most of the T range, the electrical resistivity $\rho \equiv RWt/L$ (here W and L are the width and length of the Hall bar, respectively, and t is the film thickness) displays a logarithmic temperature dependence, increasing by approximately 30 $\mu\Omega$ m per decade in T. The data for the main panel in Fig. 1 are taken in two separate cryostats to span the full T range. Notably, ρ changes monotonically from room temperature down to $T^* \approx 0.2$ K, below which the dependence begins to flatten

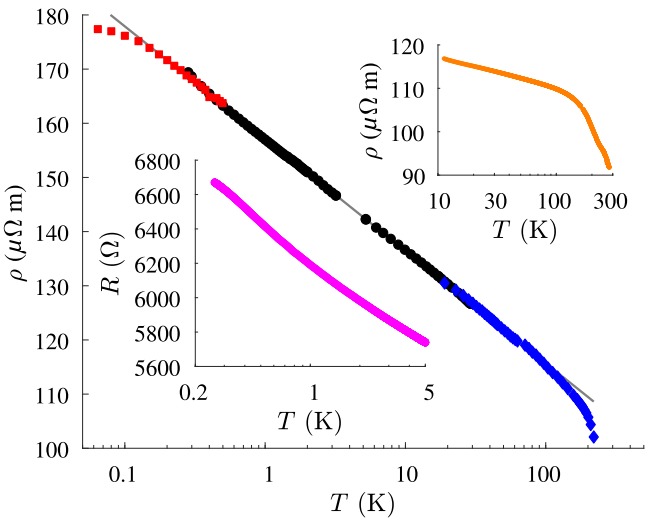

FIG. 1. Resistivity (ρ) versus temperature (T) for a Au_xGe_{1-x} film ($x = 0.07$). The Au_xGe_{1-x} film shows a monotonic decrease in ρ from 0.2 K all the way up to room temperature, thus behaving as a thermistor over a very wide T range. The behavior up to approximately 200 K is described well by a logarithmic equation as explained in the main text. Different markers correspond to measurements taken in different cryostats or while cooling, normalized by multiplicative factors of 1%–2%. The solid line shows a fit to the data shown in black circles. The top inset (orange curve) shows measurements on another Au_xGe_{1-x} sample ($x \approx 0.1$), taken while cooling from room temperature. The bottom inset (magenta curve) shows $R(T)$ measurements for a Au_xGe_{1-x} ($x = 0.07$) film grown on a sapphire substrate, taken in a third cryostat while T is ramped continuously. The Au_xGe_{1-x} alloy can be used as a single sensor operable between 0.2 and 200 K.

out. Above T^*, $d\rho/d\log T$ is constant [and so $\rho(\log T)$ is linear] until approximately 200 K, where there is a distinct change in slope. Between these limits the data are fitted to

$$\rho(T) = -\rho_0 \log\left(\frac{T}{T_0}\right), \tag{1}$$

where ρ_0 and T_0 are fitting parameters depending on the exact composition of the alloy.

Not only is the logarithmic form of $\rho(T)$ applicable over a wide T range, but ρ also shows little deviation from this functional form. This accuracy in the form of $\rho(T)$ should make this material useful for R-based thermometry, as any deviations adversely impact the accuracy of the measured T. Furthermore, the simplicity and accuracy of Eq. (1) make calibration straightforward. Calibrating a $Au_{0.07}Ge_{0.93}$ thermometer would require measurements at only two well-defined values of T; for example, when the thermometer is immersed in liquid nitrogen and in liquid helium. More calibration points could improve the calibration and/or extend the T range over which the thermometer is calibrated.

The relatively straightforward calibration offsets an unexpected cool-down dependence of R. As shown in Fig. S3 [27], we observe a nonsystematic variation of R between cool downs. While this effect is small, it is certainly within experimental resolution. The origin of this effect is unexplained as of now, and may have to do with the differential thermal expansion of the film with respect to the substrate. However, we can rule out the role of atomic diffusion as the resistance of the samples is stable when they stored at room temperature for several weeks or months. Likewise, the resistance does not vary when the samples are maintained at subkelvin temperatures, implicating the temperature change as responsible for the observed cool-down dependence. We notice that encapsulating the film in a few hundred nanometers of Ge substantially increases the stability. However, even in the absence of capping, a simple two-point calibration should mitigate the error introduced by this variation.

Figure 2 shows that down to $T \approx 0.2$ K the sensitivity $S \equiv dR/dT$ of the $Au_{0.07}Ge_{0.93}$ alloy as a thermometer increases as $T \to 0$ K. Although this dependence is found even in semiconductor materials, in those the advantage gained due to the increasing S is offset by the correspondingly large values of R. This is the primary difference between semiconductors and the Au_xGe_{1-x} alloy, in which the absolute value of R remains moderate. Therefore, we examine not only S but also the "dimensionless sensitivity" $T/R\ dR/dT$, which, importantly, is found to vary by less than a factor of 2 over 3 decades in T. This is to be contrasted with the behavior of commercially available thermometers, in which the dimensionless sensitivity typically varies by more than 1 order of magnitude over comparable T scales, restricting the T range over which they can be used [15]. The weak dependence of the dimensionless sensitivity on T suggests not only that a single sensor element can be used over a wide T range but also that the same electronic instrument required to measure R can be used over the whole T range.

It is instructive to consider how the fractional error in a temperature reading varies with temperature. Normally, the dimensionless sensitivity gives an indication of this, assuming that the fractional error in the resistance measurement remains constant throughout the T range of operation. However, since ρ of the Au-Ge film changes only relatively slowly with temperature, changing by less than 1 order of magnitude over the entire T range studied, it is reasonable to consider the case of resistance measurements having a fixed uncertainty σ_R over the entire temperature range. With use of Eq. (1), this leads to an uncertainty in the measured T of $\sigma_T \sim T\sigma_R$. Over the entire range of applicability of Eq. (1) the fractional uncertainty in the temperature measurement is therefore constant. Therefore, the Au-Ge alloys described here have the potential to be used to make thermometers that are equally useful at low and relatively high T.

We now explore how changing the composition affects the behavior of the material. A similar logarithmic $\rho\,(T)$ dependence is observed in samples with a variety of compositions of Au_xGe_{1-x} $(0.07 \le x \le 0.21)$. Figure 3 shows

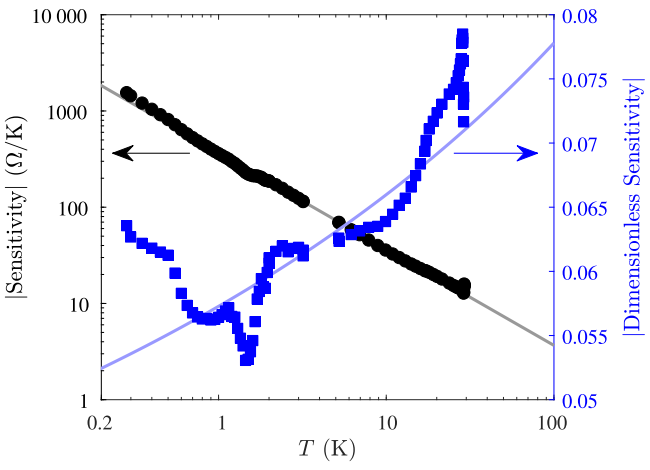

FIG. 2. Sensitivity $S \equiv dR/dT$ (left axis, black circles) and dimensionless sensitivity $T/R\ dR/dT$ (right axis, blue squares) for the $Au_{0.07}Ge_{0.93}$ sample. The $1/T$ dependence (solid line) of S is consistent with the logarithmic behavior of $R(T)$. The dimensionless sensitivity varies by only approximately 60% over nearly 3 orders of magnitude in T. Here the points are extracted by our numerically differentiating the data, whereas the solid lines are calculated from the fit shown in Fig. 1.

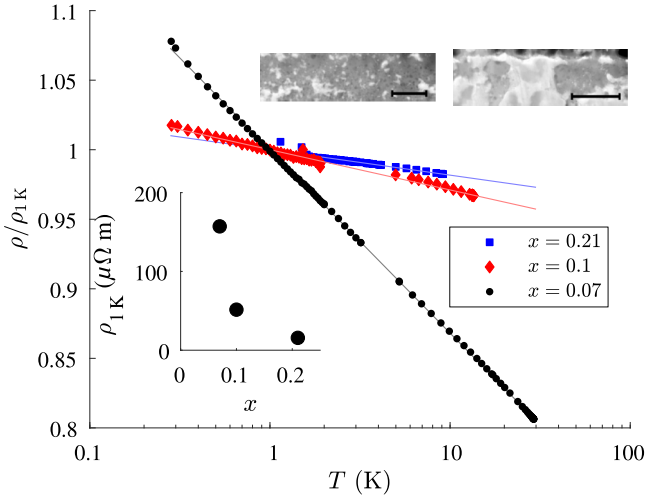

FIG. 3. $\rho(T)$ for three Au_xGe_{1-x} compositions. The main panel shows $\rho(T)/\rho(1\text{ K})$ for different compositions and the solid lines show the respective logarithmic fits. The bottom inset shows $\rho(x)$ at 1 K. The top insets show cross-section TEM images of $Au_{0.07}Ge_{0.93}$ (left) and $Au_{0.21}Ge_{0.79}$ (right), in which the brighter regions are Au richer. The scale bar in each image represents 200 nm. The resistivity as measured between different pairs of contacts is consistent, suggesting that the disorder that exists on short length scales is averaged out in the macroscopically large devices studied here.

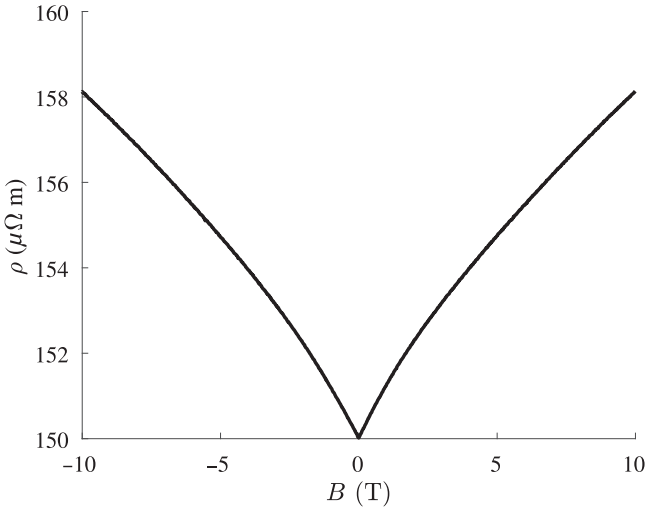

FIG. 4. $\rho(B)$ of $Au_{0.07}Ge_{0.93}$ at 1.8 K. The high-field magnetoresistance is approximately linear.

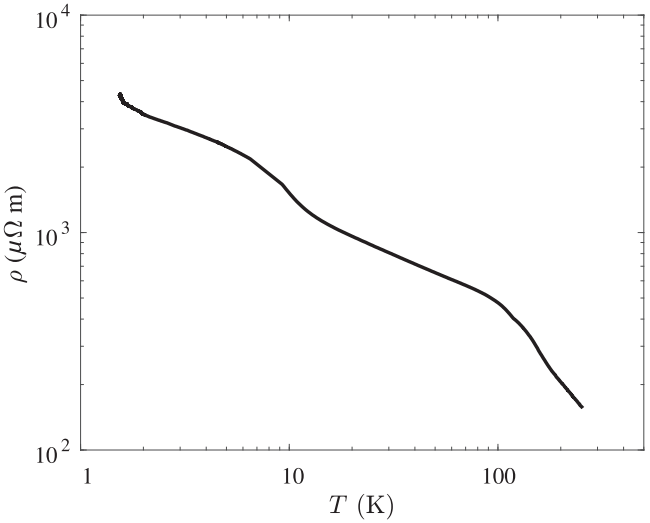

FIG. 5. $\rho(T)$ for a $Au_{0.07}Ge_{0.93}$ film heated at approximately 250 °C after deposition does not have a logarithmic T dependence but has an approximately power-law dependence. Furthermore, the absolute values of ρ are significantly larger than in otherwise identical samples heated to approximately 450 °C (Fig. 1).

that S is the largest for $x = 0.07$, for which the uncertainties in the fitting parameters are also the smallest. While this suggests that both S and the accuracy may be increased by further reducing x, we also note that this would increase the absolute value of ρ.

What is the response of the Au_xGe_{1-x} alloy to a magnetic field B? As shown in Fig. 4, for $T \gtrsim 1$ K the films show an approximately linear magnetoresistance at high B [16–18], with weak antilocalization at small B. This allows, in principle, a simple calibration-based readout of T in the presence of a finite B. We also note that at 1.8 K the magnetoresistance is approximately 0.5%/T, implying that the induced error is approximately 0.13 K/T. Below 1 K, the B response of Au_xGe_{1-x} becomes more complex, with $\rho(B)$ showing nonmonotonic behavior and slow transients similar to that reported in Refs. [19,20].

The postdeposition heat treatment of the Au_xGe_{1-x} alloy has a crucial impact on its performance as a thermometer. Figure 5 shows $\rho(T)$ for a sample of $Au_{0.07}Ge_{0.93}$, with the material deposited at the same time as for the sample corresponding to Fig. 1, but importantly with the only difference being that it is annealed at 250 °C, which is below the eutectic point T_E of Au-Ge alloys (approximately 360 °C) [21]. The sample corresponding to Fig. 5 does not show a logarithmic $\rho(T)$, but instead the dependence is closer to a power-law dependence, consistent with previous work that suggested the use of Au_xGe_{1-x} alloys as thermometers, where the films were heated at $T < T_E$ [22]. Clearly, the overall characteristics are far less satisfactory in terms of how sensitivity and accuracy vary with temperature compared with those shown in Fig. 1.

The observed logarithmic $\rho(T)$ is clearly correlated to the heat treatment of the films. Cochrane *et al.* [23] reported logarithmic dependences of ρ on T in *moderately* disordered materials and explained their findings on the basis of disorder-induced, nonmagnetic localized microscopic degrees of freedom, which act as sources for Kondo-type scattering events. These localized degrees of freedom correspond to different configurations of atomic positions that are separated by potential wells and have a finite tunneling amplitude. Unlike in the case of localized magnetic spins, the resulting eigenstates are not perfectly degenerate, but instead have their energy levels split by Δ. This gives a resistance dependence of

$$\rho \propto -\log\left[\left(\frac{k_B T}{D}\right)^2 + \left(\frac{\Delta}{D}\right)^2\right], \tag{2}$$

where D is the electron bandwidth. Consequently, the logarithmic behavior ceases when $k_B T \lesssim \Delta$, and ρ becomes independent of T.

The visibly disordered character of the Au_xGe_{1-x} films suggests that the observed logarithmic $\rho(T)$ arises due to similar physics, as indicated by the TEM images (inset in Fig. 3), which reveal that the films are phase separated. Consideration of the phase diagram [21] suggests that the two phases are Au-rich islands (containing approximately 30% Ge) and an almost pure Ge matrix. This is consistent with energy-dispersive-x-ray-spectroscopy measurements. Generally, it is observed that as the fraction of Au is decreased, the logarithmic fit for $\rho(T)$ becomes better (Fig. 3), and this might suggest that the logarithmic conductivity arises dominantly through the Ge matrix. In samples with large contiguous regions of Au-rich material, conduction through the Au-rich regions becomes more important, and causes a correction of the $\rho(T)$ dependence.

We speculate that the Ge matrix is slightly disordered, presumably due to the rapid cooling after the heat treatment and/or the presence of Au impurities that disturb the crystallinity. The flattening of $\rho(T)$ at low T (Fig. 1) suggests that $\Delta \approx 0.2\ \mathrm{K} \times k_B$ in the Au_xGe_{1-x} films. The observed "shoulder" in $\rho(T)$ at $T \approx 200$ K is also consistent with the observations in Ref. [23], and we speculate that these can arise due to higher energy levels of the Kondo-type scattering center. Notably, over the explored T range we see no indication of a minimum in $\rho(T)$, which is expected at a certain temperature, depending on the concentration of Kondo-type scatterers [24]. Separately, we also note that the observed linear magnetoresistance (Fig. 4) is consistent with the picture of microscopic disorder playing a pivotal role in the transport, as linear magnetoresistance is characteristic of disordered materials [16–18].

We note that there are other possible sources of a logarithmic temperature dependence, such as granular systems [25] and thin disordered films [26], but these apply to electrical conductivity rather than resistivity as seen here. As shown in Fig. S4 [27], $\rho(T)$ clearly fits a log T dependence more consistently.

IV. CONCLUSION

In conclusion, we present a Au_xGe_{1-x} alloy with clear practical advantages for simple R-based thermometry from room temperature down to approximately 0.2 K. Principally, the use of a *single sensor* over this T range eliminates the necessity of matching calibrations of different thermometers at the limits of their applicability, while also reducing costs for multiple sensors and the associated wiring and measurement apparatus. Furthermore, the reasonably low values of R over the entire T range alleviate the need for apparatus that can measure R with high precision and without appreciable self-heating. The possibility of lithographically patterning the alloy suggests that micrometer-scale thermometers can be deposited directly onto substrates of choice, allowing thermal and thermoelectric measurements on small samples and at low T. The accuracy of the logarithmic T dependence over a wide T range allows a simple two-point calibration. We find that the characteristic logarithmic $\rho(T)$ behavior of the alloy is linked to its composition and the precise conditions of preparation, in particular annealing above the eutectic temperature. We suggest that the mechanism driving the logarithmic resistance dependence on temperature is the same as that reported previously in moderately disordered metallic alloys; namely, where the disorder induces Kondo-like scattering centers. Strikingly, however, the T range over which we observe the logarithmic behavior is significantly larger than in any previous report we are aware of, with the anticipated "upturn" in resistance not occurring up to room temperature.

ACKNOWLEDGMENTS

J.R.A.D., P.C.V., G.J.C., and V.N. acknowledge funding from the Engineering and Physical Sciences Research Council, United Kingdom. G.J.C. and S.E.R. acknowledge funding from the Royal Society, United Kingdom. J.F.O. thanks the Brazilian Agency CNPq. A.D. and S.K-N. acknowledge financial support through a European Research Council Starting Grant (Grant No. ERC-2014-STG-639526, NANOGEN). We thank J.J. Rickard for support with TEM.

[1] H. Marshak, Nuclear orientation thermometry, J. Res. Natl. Bur. Stand. (1934) **88**, 175 (1983).
[2] G. Schuster, D. Hechtfischer, and B. Fellmuth, Thermometry below 1 K, Rep. Progr. Phys. **57**, 187 (1994).
[3] L. Spietz, K. W. Lehnert, I. Siddiqi, and R. J. Schoelkopf, Primary electronic thermometry using the shot noise of a tunnel junction, Science **300**, 1929 (2003).
[4] D. R. White, R. Galleano, A. Actis, H. Brixy, M. De Groot, J. Dubbeldam, A. L. Reesink, F. Edler, H. Sakurai, R. L. Shepard, and J. C. Gallop, The status of Johnson noise thermometry, Metrologia **33**, 325 (1996).
[5] J. P. Pekola, K. P. Hirvi, J. P. Kauppinen, and M. A. Paalanen, Thermometry by Arrays of Tunnel Junctions, Phys. Rev. Lett. **73**, 2903 (1994).
[6] J. P. Kauppinen, K. T. Loberg, A. J. Manninen, J. P. Pekola, and R. A. Voutilainen, Coulomb blockade thermometer: Tests and instrumentation, Rev. Sci. Instrum. **69**, 4166 (1998).
[7] W. N. Lawless, A low temperature glass-ceramic capacitance thermometer, Rev. Sci. Instrum. **42**, 561 (1971).
[8] W. E. Chickering, J. P. Eisenstein, and J. L. Reno, Hot-Electron Thermocouple and the Diffusion Thermopower of Two-Dimensional Electrons in GaAs, Phys. Rev. Lett. **103**, 046807 (2009).
[9] V. Narayan, M. Pepper, J. Griffiths, H. Beere, F. Sfigakis, G. Jones, D. Ritchie, and A. Ghosh, Unconventional metallicity and giant thermopower in a strongly interacting two-dimensional electron system, Phys. Rev. B **86**, 125406 (2012).
[10] J. Billiald, D. Backes, J. König, I. Farrer, D. Ritchie, and V. Narayan, Determining energy relaxation length scales in two-dimensional electron gases, Appl. Phys. Lett. **107**, 022104 (2015).
[11] V. Narayan, E. Kogan, C. Ford, M. Pepper, M. Kaveh, J. Griffiths, G. Jones, H. Beere, and D. Ritchie, Density-dependent thermopower oscillations in mesoscopic two-dimensional electron gases, New J. Phys. **16**, 085009 (2014).
[12] A. Mavalankar, S. J. Chorley, J. Griffiths, G. A. C. Jones, I. Farrer, D. A. Ritchie, and C. G. Smith, A non-invasive electron thermometer based on charge sensing of a quantum dot, Appl. Phys. Lett. **103**, 133116 (2013).
[13] A. V. Feshchenko, L. Casparis, I. M. Khaymovich, D. Maradan, O.-P. Saira, M. Palma, M. Meschke, J. P. Pekola,

and D. M. Zumbühl, Tunnel-junction Thermometry Down to Millikelvin Temperatures, Phys. Rev. Appl. **4**, 034001 (2015).

[14] O.-P. Saira, M. Zgirski, K. L. Viisanen, D. S. Golubev, and J. P. Pekola, Dispersive Thermometry with a Josephson Junction Coupled to a Resonator, Phys. Rev. Appl. **6**, 024005 (2016).

[15] Lake Shore Cernox RTDs, https://www.lakeshore.com/Documents/LSTC˙Cernox˙l.pdf (accessed: 2018-04-12).

[16] Y. A. Dreizin and A. M. Dykhne, Anomalous conductivity of inhomogeneous media in a strong magnetic field, Sov. Phys. JETP **36**, 127 (1973).

[17] D. Stroud and F. P. Pan, Effect of isolated inhomogeneities on the galvanomagnetic properties of solids, Phys. Rev. B **13**, 1434 (1976).

[18] M. M. Parish and P. B. Littlewood, Classical magnetotransport of inhomogeneous conductors, Phys. Rev. B **72**, 094417 (2005).

[19] V. Narayan, P. C. Verpoort, J. R. A. Dann, D. Backes, C. J. B. Ford, M. Lanius, A. R. Jalil, P. Schüffelgen, G. Mussler, G. J. Conduit, and D. Grützmacher, Long-lived nonequilibrium superconductivity in a noncentrosymmetric Rashba semiconductor, Phys. Rev. B **100**, 024504 (2019).

[20] P. C. Verpoort and V. Narayan, Slowly-decaying chirality states in low-temperature strongly rashba-coupled systems, arXiv:1902.04678 (2019).

[21] H. Okamoto and T. B. Massalski, The Au-Ge (gold-germanium) system, Bull. Alloy Phase Diagrams **5**, 601 (1984).

[22] O. Béthoux, R. Brusetti, J. C. Lasjaunias, and S. Sahling, Au-Ge film thermometers for temperature range 30 mK–300 K, Cryogenics **35**, 447 (1995).

[23] R. W. Cochrane, R. Harris, J. O. Ström-Olson, and M. J. Zuckermann, Structural Manifestations in Amorphous Alloys: Resistance Minima, Phys. Rev. Lett. **35**, 676 (1975).

[24] J. Kondo, Resistance minimum in dilute magnetic alloys, Progr. Theor. Phys. **32**, 37 (1964).

[25] I. S. Beloborodov, A. V. Lopatin, V. M. Vinokur, and K. B. Efetov, Granular electronic systems, Rev. Mod. Phys. **79**, 469 (2007).

[26] P. A. Lee and T. V. Ramakrishnan, Disordered electronic systems, Rev. Mod. Phys. **57**, 287 (1985).

[27] See Supplemental Material at http://link.aps.org/supplemental/10.1103/PhysRevApplied.12.034024 for graphs related to fabrication, materials characterisation, cooldown variation, and contrast between resistance and conductance.